NASA Contractor Report 189171

Users Manual for Updated Computer Code for Axial-Flow Compressor Conceptual Design

Arthur J. Glassman
University of Toledo
Toledo, Ohio

July 1992

Prepared for
Lewis Research Center
Under Grant NAG3-1165

National Aeronautics and
Space Administration

USERS MANUAL FOR UPDATED COMPUTER CODE FOR AXIAL-FLOW COMPRESSOR CONCEPTUAL DESIGN

Arthur J. Glassman*
The University of Toledo
Toledo, Ohio 43606

SUMMARY

An existing computer code that determines the flow path for an axial-flow compressor either for a given number of stages or for a given overall pressure ratio was modified for use in air-breathing engine conceptual design studies. This code uses a rapid approximate design methodology that is based on isentropic simple radial equilibrium. Calculations are performed at constant-span-fraction locations from tip to hub. Energy addition per stage is controlled by specifying the maximum allowable values for several aerodynamic design parameters.

New modeling was introduced to the code to overcome perceived limitations. Specific changes included variable rather than constant tip radius, flow path inclination added to the continuity equation, input of mass flow rate directly rather than indirectly as inlet axial velocity, solution for the exact value of overall pressure ratio rather than for any value that met or exceeded it, and internal computation of efficiency rather than the use of input values. The modified code was shown to be capable of computing efficiencies that are compatible with those of five multistage compressors and one fan that were tested experimentally.

This report serves as a users manual for the revised code, which is named CSPAN, an acronym for Compressor SPanline ANalysis. The modeling modifications, including two internal loss correlations, are presented. Program input and output are described. A sample case for a multistage compressor is included.

INTRODUCTION

Performing engine studies requires the capability to produce conceptual designs of the components in order to determine geometry, performance, and weight. One major component of air-breathing turbine engines is the compressor. The typical compressor "design" code enables a study of the interrelationship of the number of stages, the flow path radii, the gas velocities, the flow angles, and the resultant variation of compressor efficiency. A computer code capable of performing this function in a rapid approximate manner was selected as being consistent with the needs of engine conceptual design. This code (ref. 1), which is based on isentropic simple radial equilibrium, was one of four compressor analysis codes developed under NASA contract about 25 years ago. The other three codes, two design (refs. 2 and 3) and one off-design (ref. 4), were streamline analyses accounting for full radial equilibrium.

An evaluation of the reference 1 code indicated several limitations to its usefulness for the conceptual sizing of engine compressors. The design was restricted to a constant tip radius, and flowpath inclination was not accounted for in the continuity calculation. In addition, the user was unable to directly specify a mass flow rate or an exact overall pressure ratio. Finally, stage efficiency had to be

*Resident Research Associate—NASA Lewis Research Center, Cleveland, Ohio.

estimated beforehand because it was a required input, and there was no provision for inlet guide vane loss. Consequently, the code was modified to overcome these deficiencies.

This report serves as a users manual for the revised code, which is named CSPAN, an acronym for Compressor SPanline ANalysis. The modeling changes are presented herein. Computed efficiencies are compared with test results from five multistage compressors and one fan. Program input and output are described. A sample case for a multistage compressor is included.

SYMBOLS

B	coefficient in tangential velocity equation (eq.(2)), (ft)(in.)/sec
b	axial distance between calculation stations, ft
C	coefficient in tangential velocity equation (eq.(2)), ft/sec
D	coefficient in tangential velocity equation (eq.(2)), ft/(sec)(in.)
D	diffusion factor
E	coefficient in tangential velocity equation (eq.(2)), ft/(sec)(in.^{2})
f	fraction of span height
g	gravitational constant, 32.17 (lbm)(ft)/(lbf)(sec^2)
H	enthalpy, Btu/lb
J	conversion constant, 778 (ft)(lb)/Btu
k	loss coefficient multiplier
M	Mach number
n	stage number
P	pressure, psi
R	radius, ft
T	temperature, $^\circ$R
U	blade speed, ft/sec
V	velocity, ft/sec
w	mass flow rate, lb/sec
z	loss function
α	angle of inclination of flow or endwalls in meridional plane, deg
β	flow angle on conical blade-to-blade surface, deg
η	efficiency
ρ	density, lb/ft^3
σ	solidity
ω	pressure-loss coefficient

Subscripts:

avg	average
cor	corrected
e	equivalent
ex	exit
g	geometric
H	hub
id	ideal
in	inlet
inp	input
ns	normal shock
ov	overall
p	polytropic
pr	profile
R	rotor
S	stator
s	static
sh	shock
stg	stage
T	tip
t	total
z	meridional component
θ	tangential component
1	rotor inlet
2	rotor exit
2D	two dimensional
3	stator exit
3D	three dimensional

Superscripts:

$'$	relative
*	uncorrected value

METHOD OF ANALYSIS

The computer code of reference 1 was developed for making parametric studies of advanced multistage axial-flow compressors. This code determines the meridional flow path for given design specifications of either the number of stages or the overall pressure ratio. Such a flow path is illustrated in figure 1(a), where the stage station locations and some of the geometry variables are defined. A typical stage velocity diagram including the symbols for all velocities and angles is shown in figure 1(b).

The flow-physics model and the solution procedure are described in detail in reference 1. These are briefly summarized herein, and then the revisions made to improve the code's usefulness for air-breathing engine conceptual design studies are described.

Flow-Physics Model

The radial equation of motion is based on isentropic simple radial equilibrium (no effects of streamline slope and curvature and radially constant entropy). Consequently, at each axial station

$$gJ\frac{dH_t}{dR} = \frac{V_\theta}{R} + \frac{d(RV_\theta)}{dR} + V_z\frac{dV_z}{dR} \tag{1}$$

where the variation of tangential velocity with radius is

$$V_\theta = \frac{B}{R} + C + DR + ER^2 \tag{2}$$

Equations (1) and (2) along with continuity

$$w = 2\pi\int_{R_H}^{R_T}\rho V_z R\,dR \tag{3}$$

and stage energy addition

$$gJ\,\Delta H_t = \Delta(UV_\theta) \tag{4}$$

provide the basic flow-physics model.

Stage energy addition is determined either by specifying the tangential velocities (eq. (2)) at both the rotor inlet and exit or by specifying the tangential velocity at the rotor inlet, the axial velocity ratio across the rotor tip, and a maximum value for the rotor tip diffusion factor,

$$D_{R,T} = 1 - \frac{V_2'}{V_1'} + \frac{V_{\theta,1}' - V_{\theta,2}'}{2\sigma V_1'} \tag{5}$$

from which rotor-exit tangential velocity is obtained. In either case, the energy addition is reduced if limit values are exceeded for stator-inlet hub Mach number, stator hub diffusion factor, or rotor-exit hub relative flow angle. Energy addition is then related to rotor and stage pressure ratios by input values of rotor and stage polytropic efficiencies, respectively.

Computation proceeds stage by stage until either a given number of stages is reached or a given overall pressure ratio is met or exceeded. The flow path geometry evolves from the given inlet tip radius and continuity and the specified limits for hub and tip ramp angles. Tip radius normally remains constant and hub radius is computed. If the hub ramp angle limit is exceeded, the tip radius is reduced so that the hub ramp angle is at its limit value.

Code Revisions

The code of reference 1 was evaluated for application to the conceptual design of compressors for air-breathing engines. These conceptual designs serve as the basis for estimating engine weight and performance. It was found that the code's usefulness could be improved by revising some of its physical modeling and solution procedures. The basic flow-physics modeling and energy-addition modeling were retained as previously described except for the inclusion of flow path inclination in the continuity equation (eq. (3)) as discussed later in this section. All modeling changes are described in this section.

Tip radius.—With the original methodology the compressor design was executed with a constant tip radius unless a hub ramp angle constraint was exceeded. Many advanced designs require tip radius reductions in order to provide adequate blade height at the exit. Therefore, an input was added to the code that allowed direct specification of the tip radius change across each blade row. The hub ramp angle limit was kept as a constraint in order to avoid excessive wall slope and if exceeded would result in further tip radius reduction.

Continuity.—In the original model the velocity is expressed in terms of two components

$$V^2 = V_z^2 + V_\theta^2 \tag{6}$$

The V_z term is referred to as "axial" velocity and is used as such for continuity (eq. (3)) even though there can be significant inclination in parts of the flow path (especially in the hub region of the inlet stages). As used in equation (6), V_z is actually a meridional velocity (the resultant of axial and radial components). Considering V_z as a meridional velocity herein, the continuity equation is revised to

$$w = 2\pi \int_{R_H}^{R_T} \rho V_Z \cos \alpha \; R \; dR \tag{7}$$

The streamline angle of inclination α is estimated as the slope of the constant-span-fraction line through the previous blade row.

Mass flow rate.—The original code required as input a value for inlet tip axial velocity, which was then used to compute a mass flow rate for the compressor. Because mass flow rate is usually specified for an engine, it is preferable to use it rather than inlet axial velocity as the input. Therefore, the calculation procedure was modified to enable a mass flow rate to be input and an iteration to be performed to find the value of inlet tip axial velocity that provided the given mass flow rate.

Overall pressure ratio.—With the original code the analysis proceeded stage by stage either until a given number of stages was reached or until a given pressure ratio was met or exceeded. This procedure did not provide an exact solution for the given overall pressure ratio. Therefore, the code was modified so that convergence to the exact specified pressure ratio can be achieved. This is done by maintaining the number of stages constant once the specified pressure ratio is exceeded and then reducing the maximum allowable rotor-blade loading (i.e., the rotor-exit tangential velocity) for all stages until the desired overall pressure ratio is obtained.

Rotor hub turning.—One of the aerodynamic constraints for a design is the amount of turning at the rotor hub. In the original code this was specified by an input value for rotor-exit hub relative flow angle. An appropriate limit value for this variable, however, is a function of the specific design. In order to generalize this constraint, it was changed to a direct input specification of rotor hub turning angle.

Inlet guide vane loss.—Computations are begun at the rotor inlet and therefore do not include the inlet guide vanes. Although a tangential velocity distribution can be specified at the first-rotor inlet (to simulate the exit flow from the inlet guide vanes), there is no way to include the inlet guide vane pressure loss as part of the compressor overall pressure ratio. In order to avoid accounting for this loss by artificially reducing compressor inlet pressure and increasing overall pressure ratio, a pressure-loss fraction $\Delta P/P$ for the inlet guide vanes was added to the input and included as part of the overall pressure ratio.

Internal loss correlations.—In the original code, rotor and stage polytropic efficiencies, which were assumed to be radially constant, had to be specified as input for each stage. As a consequence there was no assurance of compatibility of the input values with the stage loading or the blade-element aerodynamics. Therefore, two loss correlations were added to the code for optional use: one for stage polytropic efficiency and the other for blade-element, pressure-loss coefficient. For engine conceptual design studies the stage polytropic efficiency correlation is recommended.

Stage polytropic efficiency: Axial-flow compressor efficiency correlations (unpublished) that are used at NASA Lewis Research Center for engine cycle studies are presented in figure 2. Stage polytropic efficiency is plotted against stage pressure ratio in figure 2(a) for current- and advanced-technology axial-flow compressor stages. The advanced-technology curve represents the improvement that is anticipated over the next 10 to 20 years. Shown in figure 2(b) is the efficiency correction for small compressors (i.e., for low values of corrected mass flow rate). The curves of figure 2 were fit with the following equations: For current-technology stages the equation for pressure ratios of 2 or less is

$$\eta^*_{p,stg} = 0.054795\left(\frac{P_3}{P_1}\right)^2 - 0.25337\left(\frac{P_3}{P_1}\right) + 1.1477 \tag{8}$$

A linear extrapolation is used beyond a stage pressure ratio of 2 to yield

$$\eta^*_{p,stg} = -0.03419\left(\frac{P_3}{P_1}\right) + 0.9285 \tag{9}$$

For advanced-technology stages the equation for pressure ratios of 2 or less is

$$\eta^{*}_{p,stg} = 0.047322\left(\frac{P_3}{P_1}\right)^2 - 0.21668\left(\frac{P_3}{P_1}\right) + 1.1241 \tag{10}$$

An extrapolation beyond a stage pressure ratio of 2 yields

$$\eta^{*}_{p,stg} = -0.027392\left(\frac{P_3}{P_1}\right) + 0.93478 \tag{11}$$

For corrected mass flow rates of less than 10 lb/sec, efficiency is reduced to account for size effects (clearances, surface finish, etc.). The size correction for corrected mass flow rates between 1.5 and 10 lb/sec is

$$\Delta\eta_{p,stg} = 0.56826\times10^{-3}\, w_{cor} - 0.62224\times10^{-3} - \frac{0.050603}{w_{cor}} \tag{12}$$

and linear extrapolation for flow rates below 1.5 lb/sec yields

$$\Delta\eta_{p,stg} = 0.01767\, w_{cor} - 0.06 \tag{13}$$

The corrected flow rate in equations (12) and (13) is defined as

$$w_{cor} = \frac{w\sqrt{T_{in}/518.7}}{P_{in}/14.7} \tag{14}$$

After correcting for size, the resultant value of stage polytropic efficiency can be adjusted by an input loss multiplier as follows:

$$\eta_{p,stg} = 1 - k_{inp}\left[1 - (\eta^{*}_{p,stg} + \Delta\eta_{p,stg})\right] \tag{15}$$

Assuming that two-thirds of the stage loss occurs in the rotor, the rotor polytropic efficiency is

$$\eta_{p,R} = 1 - \frac{2}{3}(1 - \eta_{p,stg}) \tag{16}$$

This approximation, which is based on experience, affects only the hub radius at rotor exits. Equations (8) to (16) were incorporated into the code as one optional method for computing efficiency.

Blade-element pressure loss: Another method for estimating efficiency is through the use of loss coefficients that are based on blade-element aerodynamics. Rotor and stator loss coefficients are defined as

$$\omega_R = \frac{P'_{t,2,id} - P'_{t,2}}{P'_{t,1} - P_{s,1}} \tag{17a}$$

$$\omega_S = \frac{P_{t,2} - P_{t,3}}{P_{t,2} - P_{s,2}} \tag{17b}$$

Each blade-element loss coefficient will be composed of profile loss and shock loss components.

The profile loss coefficients are obtained from two-dimensional cascade data with a correction for three-dimensional effects. Two-dimensional loss coefficient data as a function of diffusion factor (eq. (5)) were obtained from reference 5 and extrapolated by using trends from reference 2. These loss data were then fit with the curve

$$z_{2D} = \frac{\omega_{2D} \cos \beta_{ex}}{2\sigma} = 0.0065 + 0.0050566\ D + 0.027721\ D^{4.7773} \tag{18}$$

The data, extrapolation, and curve fit are presented in figure 3. The default curve-fit coefficients used for equation (18) can be replaced through program input by alternative values that match other sources of loss data.

The loss function z was then modified for three-dimensional effects on the basis of the loss data used in reference 6 as follows:

$$z_{3D} = k_{3D} z_{2D} \tag{19}$$

The three-dimensional correction k_{3D} is based on the fraction of span height from the tip

$$f = \frac{R_T - R}{R_T - R_H} \tag{20}$$

For the outer 30 percent of span ($f < 0.3$)

$$k_{3D} = 1.87 - 2.9f \tag{21a}$$

and for the inner 30 percent of span ($f > 0.7$)

$$k_{3D} = 2f - 0.4 \tag{21b}$$

There is no correction for the center 40 percent of blade span.

The profile loss function was increased by 50 percent on the basis of experimental compressor performance (see next subsection) and can be arbitrarily adjusted further by an input loss multiplier.

$$z_{pr} = 1.5 k_{inp} z_{3D} \tag{22}$$

The profile loss coefficient is then

$$\omega_{pr} = \frac{2\sigma z_{pr}}{\cos \beta_{ex}} \tag{23}$$

The shock loss coefficient is based on the methodology of reference 7, wherein the passage-shock loss is taken as the normal-shock loss from the arithmetic average of the inlet and the estimated peak suction-surface Mach numbers. The authors of reference 6 state that a shock loss so determined is excessive, and they recommend that the normal-shock loss be divided by the square of the average Mach number. Therefore, the rotor shock loss coefficient is

$$\omega_{ns} = \frac{1 - P'_{t,ns}/P'_{t,1}}{1 - P_{s,1}/P'_{t,1}} \tag{24}$$

and

$$\omega_{sh} = \frac{\omega_{ns}}{\left(M'_{avg}\right)^2} \tag{25}$$

Although a shock also can theoretically occur in the stator, aerodynamic constraints that are imposed on the design normally prevent this.

The blade-element overall loss coefficient is then

$$\omega_{ov} = \omega_{pr} + \omega_{sh} \tag{26}$$

and the blade-row exit total pressure is determined from this loss coefficient.

Comparison with experimental performance: In order to test the loss models, calculated performance was compared with experimental performance for five multistage compressors (refs. 8 to 12) and one fan (ref. 13). The overall design features of these machines are presented in table I along with estimates of the design-point efficiencies that are based on test data.

The data reported in references 8 to 13 are for research or early-development compressors and therefore are not representative of the design-point efficiency levels that are achievable in developed engines. Consequently, for the purposes of this comparison the measured design-point efficiencies of the

referenced compressors were adjusted to a projected design-point value. The projected value was taken as the maximum efficiency either at design speed or, if there appeared to be a significant mismatch at design speed, at a somewhat lower speed. This adjustment procedure is largely subjective, but there appear to be no published data on the performance of fully developed current- and advanced-technology compressors.

The referenced compressors were modeled for the CSPAN program, which was run using both loss models. The design-point efficiency comparison of calculated and measured efficiencies is presented in figure 4. For the polytropic efficiency correlation the calculated and measured efficiencies were within one point of each other for all five multistage compressors and were within two points for the fan. For the pressure-loss coefficient correlation the multiplier of 1.5 introduced into equation (22) was based on the best overall comparison between calculated and measured values. With this value, four of the compressors compared to within about one point, but the calculated efficiency of the fan was more than three points low. These loss models seem to yield reasonable estimates for multistage compressors, but some adjustment in the input loss multiplier k_{inp} may be needed for fans.

DESCRIPTION OF INPUT AND OUTPUT

This section presents a detailed description of input and output for program CSPAN. Included with the input and output is a sample case for a five-stage transonic compressor.

Input

The input, which is read on unit 05, consists of a title line and one NAMELIST dataset. Input for the sample case is presented in table II. The title, which is printed as a heading on the output file, can contain up to 71 characters located anywhere in columns 2 through 72 on the title line. A title, even if it is left blank, must be the first record of the input data.

The physical data and option switches are input in data sets having the NAMELIST name NAME. The variables that compose NAME are defined herein along with units and default values. They are presented in order as general inputs, inlet inputs, rotor inputs, and stator inputs.

General:

CP	specific heat of working fluid, Btu/(lb)($^\circ$R)
MW	molecular weight of working fluid, lb/(lb mol)
GAM	specific heat ratio
RCLIM	limit value for overall pressure ratio
NSLIM	limit value for number of stages
N	number of calculation locations from tip to hub
ICV	pressure ratio convergence switch (default = 1) 0—accepts overall pressure ratio equal to or greater than RCLIM as a solution 1—converges to overall pressure ratio equal to RCLIM

IPR1	debug output switch (default = 0) 0—no debug output 1—minimum debug output 2—extensive debug output
IPR2	station output switch (default = 0) 0—output printed for all radial locations 1—output printed for tip and hub only
DPPIGV	inlet guide vane total-pressure loss fraction (default = 0.0)
WK	loss multiplier, equation (15) or (22) (default = 1.0)
IIT	technology-level indicator for polytropic efficiency (default = 1) 1—current technology, equations (8) and (9) 2—advanced technology, equations (10) and (11)
AZ0	constant term in pressure-loss coefficient correlation, equation (18) (default = 0.0065)
AZ1	coefficient of linear term in pressure-loss coefficient correlation, equation (18) (default = 0.0050566)
AZ2	coefficient of exponential term in pressure-loss coefficient correlation, equation (18) (default = 0.027721)
AZ3	exponent in pressure-loss coefficient correlation, equation (18) (default = 4.7773)
Inlet:	
TTI	inlet total temperature, $^{\circ}R$
PTI	inlet total pressure, psi
RTIP1I	tip radius at first-rotor inlet, in.
UTIP1I	blade speed at first-rotor inlet, ft/sec
RHORT1	hub/tip radius ratio at first-rotor inlet
VZTIPO	inlet axial velocity or mass flow rate specifier >0—VZTIPO is the axial velocity at first-rotor inlet, ft/sec <0—|VZTIPO| is the mass flow rate, lb/sec
DTIP1	tip blockage factor at first-rotor inlet (default = 1.0)
DH1	hub blockage factor at first-rotor inlet (default = 1.0)
B1	coefficient B for equation (2) at first-rotor inlet, (ft)(in.)/sec
C1	coefficient C for equation (2) at first-rotor inlet, ft/sec (default = 0.0)
D1	coefficient D for equation (2) at first-rotor inlet, ft/(sec)(in.) (default = 0.0)
E1	coefficient E for equation (2) at first-rotor inlet, ft/(sec)(in.^{2}) (default = 0.0)
Rotor: Each variable requires NSLIM values.	
RT2OT1(I)	ratio of exit tip radius to inlet tip radius for each rotor (default = 1.0)
VT2OT1(I)	ratio of exit tip meridional velocity to inlet tip meridional velocity for each rotor

NPRI(I) efficiency specifier for each rotor

> 0.0—input value is rotor polytropic efficiency
= 0.0—polytropic efficiency correlation is used
= −1.0—pressure-loss coefficient correlation is used

SRTIP(I) rotor tip solidity

ARO(I) rotor aspect ratio (based on axial chord)

DTIP2(I) tip blockage factor at rotor exit (default = 1.0)

DH2(I) hub blockage factor at rotor exit (default = 1.0)

ARHD(I) rotor hub ramp angle limit, deg

ARTD(I) rotor tip ramp angle limit, deg

DRT(I) rotor tip diffusion factor maximum value

BO(I) rotor-exit tangential velocity specifier

= 0.0—rotor tip exit tangential velocity determined from rotor tip diffusion factor by equation (5)
> 0.0—coefficient B for equation (2) at rotor exit, (ft)(in.)/sec

C2(I) coefficient C for equation (2) at rotor exit, ft/sec (default = 0.0)

D2(I) coefficient D for equation (2) at rotor exit, ft/(sec)(in.) (default = 0.0)

E2(I) coefficient E for equation (2) at rotor exit, ft/(sec)(in.^{2}) (default = 0.0)

BPSD(I) limit value for rotor hub turning, deg

Stator: Each variable requires NSLIM values.

RT3OT2(I) ratio of exit tip radius to inlet tip radius for each stator (default = 1.0)

VT3OT2(I) ratio of exit tip meridional velocity to inlet tip meridional velocity for each stator

NPSI(I) efficiency specifier for each stage

> 0.0—input value is stage polytropic efficiency
= 0.0—polytropic efficiency correlation is used
= −1.0—pressure-loss coefficient correlation is used

SSH(I) stator hub solidity

ASO(I) stator aspect ratio (based on axial chord)

DTIP3(I) tip blockage factor at stator exit (default = 1.0)

DH3(I) hub blockage factor at stator exit (default = 1.0)

ASHD(I) stator hub ramp angle limit, deg

ASTD(I) stator tip ramp angle limit, deg

DSH(I) limit value for stator hub diffusion factor

MSH(I) limit value for stator hub inlet Mach number

B3(I) coefficient B for equation (2) at stator exit, (ft)(in.)/sec

C3(I) coefficient C for equation (2) at stator exit, ft/sec (default = 0.0)

D3(I) coefficient D for equation (2) at stator exit, ft/(sec)(in.) (default = 0.0)

E3(I) coefficient E for equation (2) at stator exit, ft/(sec)(in.^{2}) (default = 0.0)

Output

Program output consists of a main output file written to unit 06 and, if applicable, a brief pressure-ratio convergence file written to unit 08. The main output presents either the results of a successful design calculation or an error message indicating the nature of the failure to find a solution that is consistent with the design specifications.

Outputs corresponding to the sample input of table II are presented in tables III and IV. The pressure-ratio convergence output, shown in table III, is most useful when sent to the terminal so that a convergence problem can be immediately detected and the computation halted. Convergence problems, however, have not occurred for any of the six cases tested (table I). As shown in table III, convergence to a pressure ratio of 5 required four iterations. Shown in the output are the number of stages followed by one line for each iteration displaying the rotor tip diffusion reduction factor (DRTK), the compressor pressure ratio (CPR), and the compressor adiabatic efficiency (EFF).

The main output is presented in table IV. For brevity in displaying the output, calculations were performed at only three radial locations (N = 3), and only the data for stages 1 and 5 are included along with the overall and inlet information. The first line of output in table IV is the title; it is followed by identification of the loss model used for this case. Then, the general inputs and the inlet inputs are printed. The values displayed are clearly identified.

The next output line in table IV states that one of the aerodynamic limits, in this case the stator hub Mach number, was exceeded in the next stage, which in this case is the first stage. As a result, the rotor tip diffusion factor was reduced from its maximum allowable value until the Mach number limit was just satisfied. The consequence of this is a reduction in stage pressure ratio.

The next block of output in table IV is the data for stage 1. This includes the rotor input, the stator input, the stage performance and geometry, and the detailed aerodynamic results at the rotor inlet, the rotor exit, and the stator exit. Note that the rotor and stator input sections include the rotor and stage polytropic efficiencies, respectively, which were determined in this case from the internal correlation. Under stage output data are the overall values of pressure ratio, temperature ratio, and adiabatic efficiency followed by the stage values, which are the same since this is the first stage. Also displayed are the rotor and stator tip and hub radii, the axial lengths, and the tip and hub ramp angles. Finally, at each of the three axial stations for the stage are presented among other parameters, the temperatures and pressures, the absolute and relative velocities, the absolute and relative flow angles, the diffusion factors, and the loss coefficients at each of the radial calculation locations.

The stage data format is identical for each stage; therefore, the "STAGE DATA" output for stages 2, 3, and 4 were omitted from table IV. Shown next is the data for stage 5. The "STAGE OUTPUT DATA" show that the overall pressure ratio of 5 has been achieved with an overall efficiency of 0.8775. For this constant-tip-radius (10 in.) design, the hub radius increased from 5.0 in. at the first-rotor inlet to 8.5 in. at the last-stator exit. The last line of output states that the specified overall pressure ratio has been achieved. If the specified pressure ratio had not been achieved, the last-line message would be that the maximum number of stages had been reached.

SUMMARY OF RESULTS

An existing computer code that determines the flow path for an axial-flow compressor either for a given number of stages or for a given overall pressure ratio was selected for use in air-breathing engine conceptual design studies. This code uses a rapid approximate design methodology that is based on isentropic simple radial equilibrium. Calculations are performed at a number of constant-span-fraction locations from tip to hub at each blade-row inlet and exit. Energy addition per stage is controlled by a maximum allowable value for the rotor tip diffusion factor, which is reduced if limit values are exceeded for the stator hub inlet Mach number, the stator hub diffusion factor, or the rotor hub turning angle.

This code was modified to make it easier to use for the conceptual study of engine compressors. The rapid approximate design methodology was retained and new modeling was introduced to overcome perceived limitations. The limitations and associated modifications were as follows:

1. Unless the given hub ramp angle limit was exceeded, the tip radius had remained constant. A tip radius change for each blade row can now be specified through input.

2. The throughflow component of velocity had been assumed to be purely axial for the continuity calculation. An internally computed flow path inclination angle was added to the continuity equation.

3. Mass flow rate had been computed from an input value of inlet axial velocity. A new algorithm allows mass flow rate to be input and the proper value of inlet axial velocity to be found by iteration.

4. Any case wherein the overall pressure ratio met or exceeded the specified value had been taken to be an acceptable solution. Convergence to the exact value of overall pressure ratio can now be achieved.

5. Rotor and stage polytropic efficiencies had to be input for each stage. Two internal loss correlations were added to the code as alternative ways to specify performance: One is for the stage polytropic efficiency and the other is for the blade-element, pressure-loss coefficient. For engine conceptual design studies the stage polytropic efficiency correlation is recommended.

6. There had been no provision to include inlet guide vane pressure loss as part of the overall pressure ratio. An input pressure-loss fraction for the inlet guide vanes has been added.

The modified code was tested by comparison with five multistage compressors and one fan for which experimental data were available. The computed performance was found to be compatible with the test results.

This report serves as a users manual for the modified code, which is named CSPAN, an acronym for Compressor SPanline ANalysis. Program input and output are described. A sample case for a multistage compressor is included.

REFERENCES

1. Bryans, A.C.; and Miller, M.L.: Computer Program for Design of Multistage Axial-Flow Compressors. NASA CR-54530, 1967.

2. Creveling, H.F.; and Carmody, R.H.: Axial-Flow Compressor Design Computer Programs Incorporating Full Radial Equilibrium. Part I—Flow Path and Radial Distribution of Energy Specified (Program 2). NASA CR-54532, 1968.

3. Creveling, H.F.; and Carmody, R.H.: Axial-Flow Compressor Design Computer Programs Incorporating Full Radial Equilibrium. Part II—Radial Distribution of Total Pressure and Flow Path or Axial Velocity Ratio Specified. NASA CR-54531, 1968.

4. Creveling, H.F.; and Carmody, R.H.: Axial Flow Compressor Computer Program for Calculating Off-Design Performance. NASA CR-72427, 1968.

5. Johnsen, I.A.; and Bullock, R.O., eds. Aerodynamic Design of Axial-Flow Compressors. NASA SP-36, 1965.

6. Crouse, J.F.; and Gorrell, W.T.: Computer Program for Aerodynamic and Blading Design of Multistage Axial-Flow Compressors. NASA TP-1946, 1981.

7. Schwenk, F.C.; Lewis, G.W.; and Hartmann, M.J.: A Preliminary Analysis of the Magnitude of Shock Losses in Transonic Compressors. NACA RM-E57A30, 1957.

8. Geye, R.P.; Budinger, R.E.; and Voit, C.H.: Investigation of a High-Pressure-Ratio Eight-Stage Axial-Flow Research Compressor With Two Transonic Inlet Stages. II—Preliminary Analysis of Overall Performance. NACA RM-E53J06, 1953.

9. Kovach, K.; and Sandercock, D.M.: Experimental Investigation of a Five-Stage Axial-Flow Research Compressor With Transonic Rotors. NACA RM–E54G01, 1954.

10. Steinke, R.J.: Design of 9.271-Pressure Ratio Five-Stage Core Compressor and Overall Performance for First Three Stages. NASA TP-2597, 1986.

11. Hosney, W.M., et al.: High Pressure Compressor (ICLS/1OC) Component Performance Report. NASA CR-174955, 1985.

12. Marchant, R.D.; Howe, D.C.; and Williams, M.C.: High-Pressure Compressor Performance Report. NASA CR-182219, 1989.

13. Cline, S.J., et al.: Energy Efficient Engine Fan and Quarter-Stage Component Performance Report. NASA CR-168070, 1982.

TABLE I.—COMPRESSORS USED FOR LOSS MODEL EVALUATION

Reference	Stages	Overall pressure ratio	Tip radius, in.	Tip speed, ft/sec	Measured efficiency
8	8	10.3	10.0	1168	0.87
9	5	5.0	10.0	1100	.87
10	3	4.5	10.1	1412	.86
11	10	23.0	13.8	1495	.86
12	10	14.0	11.7	1245	.86
13	1	1.65	41.4	1350	.89

TABLE II.—SAMPLE INPUT

```
    NACA 5 STAGE TRANSONIC COMPRESSOR
&NAME
CP=.24,MW=29.,GAM=1.4,RCLIM=5.0,NSLIM=5,N=3,
TTI=518.7,PTI=14.7,RTIPII=10.,UTIPII=1100.,RHORTI=.5,VZTIPO=-67.5,BI=0.0,
VT2OTI=.918,.885,.916,.909,.916,NPRI=5*0.0,SRTIP=0.98,1.17,1.30,1.14,0.99,
ARO=2.,1.52,1.11,0.99,0.92,DRT=5*.45,BO=5*0.0,BPSD=5*45.,
VT3OT2=1.094,1.071,1.053,1.057,0.992,NPSI=5*0.0,SSH=1.8,1.9,1.6,1.5,1.4,
ASO=2.15,1.63,1.24,1.01,0.88,DSH=5*.55,MSH=5*.75,B3=5*0.0,
&END
```

TABLE III.—CONVERGENCE OUTPUT FOR SAMPLE CASE

```
STAGES=          5
DRTK=  1.00000000     CPR=  5.45497990     EFF= 0.873050213
DRTK= 0.916593611     CPR=  4.95435619     EFF= 0.877941251
DRTK= 0.924198091     CPR=  4.99855804     EFF= 0.877498388
DRTK= 0.924446106     CPR=  5.00001240     EFF= 0.877484918
```

TABLE IV.—MAIN OUTPUT FOR SAMPLE CASE

NACA 5 STAGE TRANSONIC COMPRESSOR

LOSS MODEL: INTERNAL CORRELATION FOR STAGE POLYTROPIC EFFICIENCY

*** I N L E T I N P U T D A T A ***

NO. RAD. STATIONS	NUMBER STAGES	SP. HEAT (BTU/(LB-R))	MOL. WT. (MOLES)	RATIO OF SP. HEAT	IN. TOT. TEMP. (DEG. R)	IN. TOT. PR. (PSI)	MASS AVG. TOT. PR. RATIO	IG DEL
3	5	0.2400	29.0000	1.4000	518.7000	14.7000	5.0000	0.0

*** R O T O R I N L E T I N P U T D A T A ***

TIP RADIUS (INCHES)	TIP WHEEL SPEED (FT/SEC)	HUB TO TIP RADIUS RATIO	MASS FLOW (LB/SEC)	TIP BLOCKAGE FACTOR	HUB BLOCKAGE FACTOR
10.0000	1100.0000	0.5000	67.5000	1.0000	1.0000

COEFFICIENTS IN TANGENTIAL VELOCITY EQUATION

B	C	D	E
0.0000	0.0000	0.0000	0.0000

****

*** STATOR HUB MACH NO. LIMIT VIOLATED ***

TABLE IV.—Continued.

******** S T A G E D A T A ********

STAGE NO. 1

*** ROTOR INPUT DATA ***

MERID VEL. RATIO	POLYTROPIC EFFICIENCY	SOLIDITY AT TIP	ASPECT RATIO	TIP BLOCKAGE FACTOR	HUB BLOCKAGE FACTOR	MAX ANGLE HUB TAPER (DEGREES)	MAX ANGLE TIP TAPER (DEGREES)
0.9180	0.9308	0.9800	2.0000	1.0000	1.0000	40.000	-20.000

MAX ROTOR DIF. FACTOR	MAX. TURNING ANGLE ROTOR HUB (DEGREES)	TIP RADIUS RATIO	COEFFICIENTS IN TANGENTIAL VELOCITY EQUATION B	C	D	E
0.4160	45.0000	1.000	0.0000	0.0000	0.0000	0.0000

*** STATOR INPUT DATA ***

MERID VELOCITY RATIO	STAGE POLYTROPIC EFFICIENCY	SOLIDITY AT HUB	ASPECT RATIO	TIP BLOCKAGE FACTOR	HUB BLOCKAGE FACTOR	MAX ANGLE HUB TAPER (DEGREES)	MAX ANGLE TIP TAPER (DEGREES)
1.0940	0.8963	1.8000	2.1500	1.0000	1.0000	40.0000	-20.0000

MAX. STATOR DIF. FACTOR	MAX HUB INLET MACH NUMBER	TIP RADIUS RATIO	COEFFICIENTS IN TANGENTIAL VELOCITY EQUATION B	C	D	E
0.5500	0.7500	1.000	0.0000	0.0000	0.0000	0.0000

--**-- S T A G E O U T P U T D A T A ***--**--***

MASS FLOW (LB/SEC) = 67.501

OVERALL MASS AVE. PR. RATIO	OVERALL MASS AVE. TEMP. RATIO	OVERALL MASS AVE. EFFICIENCY	MASS AVE. PRESSURE RATIO	MASS AVE. TEMPERATURE RATIO	MASS AVE. EFFICIENCY	ROTOR ASPECT RATIO	STATOR ASPECT RATIO	OVER MASS POLY
1.4423	1.1238	0.8907	1.4423	1.1238	0.8907	2.0000	2.1500	0.

ROTOR TIP RAD. 1-G (INCHES)	ROTOR HUB RAD. 1-G (INCHES)	ROTOR TIP RAD. 2-G (INCHES)	ROTOR HUB RAD. 2-G (INCHES)	STATOR TIP RAD. 3-G (INCHES)	STATOR HUB RAD. 3-G (INCHES)	ROTOR PROJ. LENGTH (INCHES)	STATOR PROJ. LENGTH (INCHES)
10.0000	5.0000	10.0000	5.8071	10.0000	6.4608	2.5000	1.9502

ROTOR TIP RAMP ANGLE (DEGREES)	ROTOR HUB RAMP ANGLE (DEGREES)	STATOR TIP RAMP ANGLE (DEGREES)	STATOR HUB RAMP ANGLE (DEGREES)
0.0000	17.8924	0.0000	18.5305

--**-- R O T O R I N L E T O U T P U T D A T A ***--**--***

STA NO.	RADIUS -E (IN)	WHEEL SPEED (FT/SEC)	MERID VEL. (FT/SEC)	TANGENT. VEL. (FT/SEC)	ABS. VEL. (FT/SEC)	REL. VEL. (FT/SEC)	ABS. AIR ANG. (DEG)	REL. AIR ANG. (DEG)	TOTAL TEMP. (DEG R)	TOTAL PRESS. (PSI)	REL. MACH NO.	ABS. MACH NO.	SHOCK LOSS COEFF	TOTAL LOSS COEFF	ROTO DIF. FACT
1	10.000	1100.000	637.702	0.000	637.702	1271.480	0.000	59.898	518.700	14.700	1.179	0.591	0.000	0.048	0.393
2	7.500	825.000	637.702	0.000	637.702	1042.731	0.000	52.297	518.700	14.700	0.967	0.591	0.000	0.065	0.456
3	5.000	550.000	637.702	0.000	637.702	842.118	0.000	40.777	518.700	14.700	0.781	0.591	0.000	0.090	0.472

--**-- R O T O R E X I T O U T P U T D A T A ***--**--***

STA NO.	RADIUS -E (IN)	WHEEL SPEED (FT/SEC)	MERID VEL. (FT/SEC)	TANGENT. VEL. (FT/SEC)	ABS. VEL. (FT/SEC)	REL. VEL. (FT/SEC)	ABS. AIR ANG. (DEG)	REL. AIR ANG. (DEG)	TOTAL TEMP. (DEG R)	TOTAL PRESS. (PSI)	SPANL INCL (DEG)	REL. MACH NO.	ABS. MACH NO.	LOSS FUNC	STA REACT
1	10.000	1100.000	585.410	350.745	682.442	950.835	30.928	51.999	582.931	21.503	0.000	0.832	0.597	0.015	0.92
2	7.904	869.391	585.410	443.781	734.606	723.774	37.165	36.018	582.931	21.503	9.170	0.637	0.646	0.021	0.82
3	5.807	638.782	585.410	603.991	841.136	586.443	45.895	3.401	582.931	21.503	17.892	0.523	0.750	0.025	0.61

--**-- S T A T O R E X I T O U T P U T D A T A ***--**--***

STA NO.	RADIUS -E (IN)	MERID VEL. (FT/SEC)	TANGENT. VEL. (FT/SEC)	ABS. VEL. (FT/SEC)	SPANL. INCL. (DEG)	ABS. AIR ANG. (DEG)	TOTAL PRESS (PSI)	SHOCK LOSS COEFF	TOTAL LOSS COEFF	STATOR DIF. FACTOR	MERID MACH NO.	ABS. MACH NO.	LOSS FUNC
1	10.000	640.438	0.000	640.438	0.000	0.000	21.201	0.000	0.065	0.294	0.558	0.558	0.030
2	8.230	640.439	0.000	640.439	9.514	0.000	21.201	0.000	0.057	0.349	0.558	0.558	0.021
3	6.461	640.439	0.000	640.439	18.530	0.000	21.201	0.000	0.045	0.438	0.558	0.558	0.013

TABLE IV.—Concluded.

******** S T A G E D A T A ********

STAGE NO. 5

*** ROTOR INPUT DATA ***

MERID VEL. RATIO	POLYTROPIC EFFICIENCY	SOLIDITY AT TIP	ASPECT RATIO	TIP BLOCKAGE FACTOR	HUB BLOCKAGE FACTOR	MAX ANGLE HUB TAPER (DEGREES)	MAX ANGLE TIP TAPER (DEGREES)
0.9160	0.9416	0.9900	0.9200	1.0000	1.0000	40.000	-20.000

MAX ROTOR DIF. FACTOR	MAX. TURNING ANGLE ROTOR HUB (DEGREES)	TIP RADIUS RATIO
0.4160	45.0000	1.000

COEFFICIENTS IN TANGENTIAL VELOCITY EQUATION

B	C	D	E
0.0000	0.0000	0.0000	0.0000

*** STATOR INPUT DATA ***

MERID VELOCITY RATIO	STAGE POLYTROPIC EFFICIENCY	SOLIDITY AT HUB	ASPECT RATIO	TIP BLOCKAGE FACTOR	HUB BLOCKAGE FACTOR	MAX ANGLE HUB TAPER (DEGREES)	MAX ANGLE TIP TAPER (DEGREES)
0.9920	0.9123	1.4000	0.8800	1.0000	1.0000	40.0000	-20.0000

MAX. STATOR DIF. FACTOR	MAX HUB INLET MACH NUMBER	TIP RADIUS RATIO
0.5500	0.7500	1.000

COEFFICIENTS IN TANGENTIAL VELOCITY EQUATION

B	C	D	E
0.0000	0.0000	0.0000	0.0000

--**-- S T A G E O U T P U T D A T A ***--**--***

MASS FLOW (LB/SEC) = 67.501

OVERALL MASS AVE. PR. RATIO	OVERALL MASS AVE. TEMP. RATIO	OVERALL MASS AVE. EFFICIENCY	MASS AVE. PRESSURE RATIO	MASS AVE. TEMPERATURE RATIO	MASS AVE. EFFICIENCY	ROTOR ASPECT RATIO	STATOR ASPECT RATIO	OVERALL MASS AVE. POLY EFF.
5.0000	1.6653	0.8775	1.2874	1.0823	0.9091	0.9200	0.8800	0.9016

ROTOR TIP RAD. 1-G (INCHES)	ROTOR HUB RAD. 1-G (INCHES)	ROTOR TIP RAD. 2-G (INCHES)	ROTOR HUB RAD. 2-G (INCHES)	STATOR TIP RAD. 3-G (INCHES)	STATOR HUB RAD. 3-G (INCHES)	ROTOR PROJ. LENGTH (INCHES)	STATOR PROJ. LENGTH (INCHES)
10.0000	8.3072	10.0000	8.4424	10.0000	8.4819	1.8400	1.7700

ROTOR TIP RAMP ANGLE (DEGREES)	ROTOR HUB RAMP ANGLE (DEGREES)	STATOR TIP RAMP ANGLE (DEGREES)	STATOR HUB RAMP ANGLE (DEGREES)
0.0000	4.2029	0.0000	1.2772

--**-- R O T O R I N L E T O U T P U T D A T A ***--**--***

STA NO.	RADIUS -E (IN)	WHEEL SPEED (FT/SEC)	MERID VEL. (FT/SEC)	TANGENT. VEL. (FT/SEC)	ABS. VEL. (FT/SEC)	REL. VEL. (FT/SEC)	ABS. AIR ANG. (DEG)	REL. AIR ANG. (DEG)	TOTAL TEMP. (DEG R)	TOTAL PRESS. (PSI)	REL. MACH NO.	ABS. MACH NO.	SHOCK LOSS COEFF	TOTAL LOSS COEFF	ROTOR DIF. FACTOR
1	10.000	1100.000	562.565	0.000	562.565	1235.506	0.000	62.914	798.105	57.093	0.908	0.413	0.000	0.039	0.416
2	9.154	1006.897	562.562	0.000	562.562	1153.394	0.000	60.807	798.105	57.093	0.847	0.413	0.000	0.043	0.451
3	8.307	913.795	562.562	0.000	562.562	1073.077	0.000	58.382	798.105	57.093	0.788	0.413	0.000	0.048	0.490

--**-- R O T O R E X I T O U T P U T D A T A ***--**--***

STA NO.	RADIUS -E (IN)	WHEEL SPEED (FT/SEC)	MERID VEL. (FT/SEC)	TANGENT. VEL. (FT/SEC)	ABS. VEL. (FT/SEC)	REL. VEL. (FT/SEC)	ABS. AIR ANG. (DEG)	REL. AIR ANG. (DEG)	TOTAL TEMP. (DEG R)	TOTAL PRESS. (PSI)	SPANL INCL (DEG)	REL. MACH NO.	ABS. MACH NO.	LOSS FUNC	STAGE REACTION
1	10.000	1100.000	515.309	358.787	627.910	902.740	34.848	55.192	863.809	74.097	0.000	0.639	0.445	0.011	0.901
2	9.221	1014.334	515.307	389.088	645.701	810.230	37.055	50.506	863.809	74.097	2.104	0.574	0.458	0.013	0.873
3	8.442	928.668	515.307	424.980	667.944	720.585	39.513	44.347	863.809	74.097	4.203	0.512	0.474	0.015	0.836

--**-- S T A T O R E X I T O U T P U T D A T A ***--**--***

STA NO.	RADIUS -E (IN)	MERID VEL. (FT/SEC)	TANGENT. VEL. (FT/SEC)	ABS. VEL. (FT/SEC)	SPANL. INCL. (DEG)	ABS. AIR ANG. (DEG)	TOTAL PRESS (PSI)	SHOCK LOSS COEFF	TOTAL LOSS COEFF	STATOR DIF. FACTOR	MERID MACH NO.	ABS. MACH NO.	LOSS FUNC
1	10.000	511.187	0.000	511.187	0.000	0.000	73.500	0.000	0.064	0.427	0.360	0.360	0.027
2	9.241	511.184	0.000	511.184	0.639	0.000	73.500	0.000	0.060	0.443	0.360	0.360	0.023
3	8.482	511.184	0.000	511.184	1.277	0.000	73.500	0.000	0.056	0.462	0.360	0.360	0.020

*** OVERALL PRESSURE RATIO LIMIT HAS BEEN REACHED -- GO TO NEW DATA ***

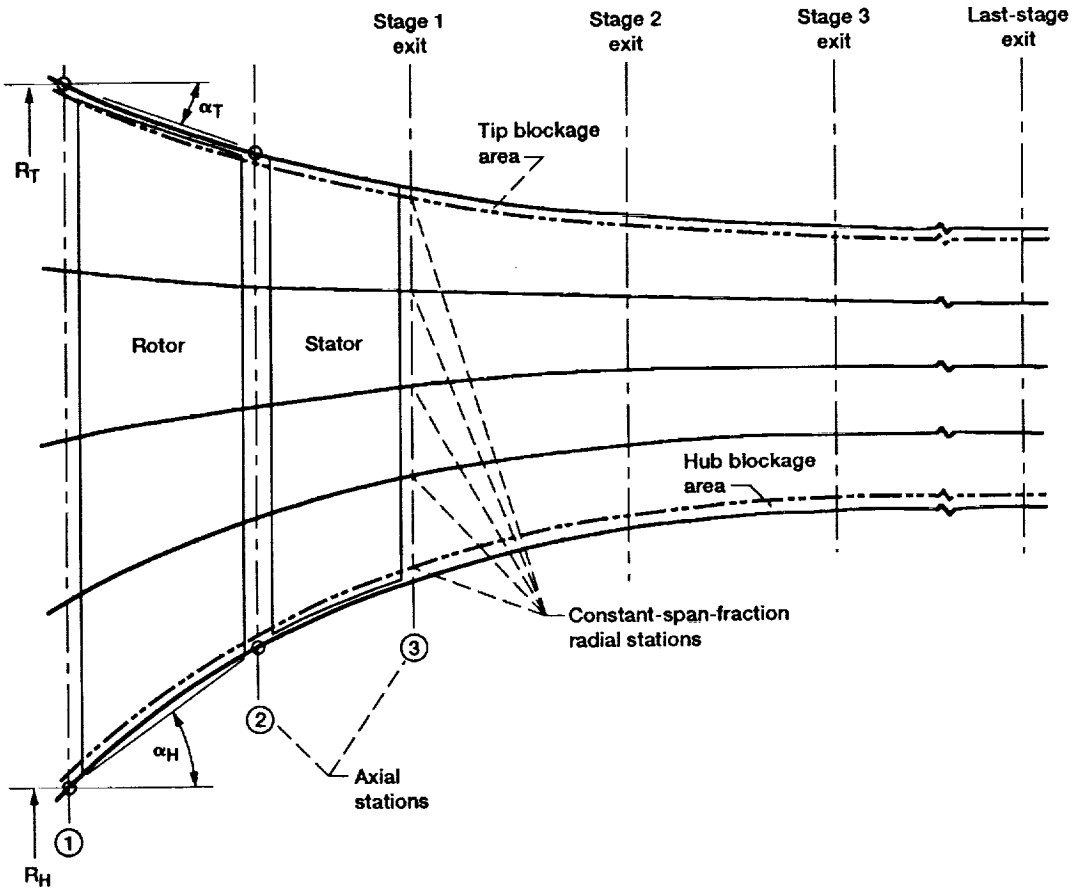

(a) Meridional flowpath.

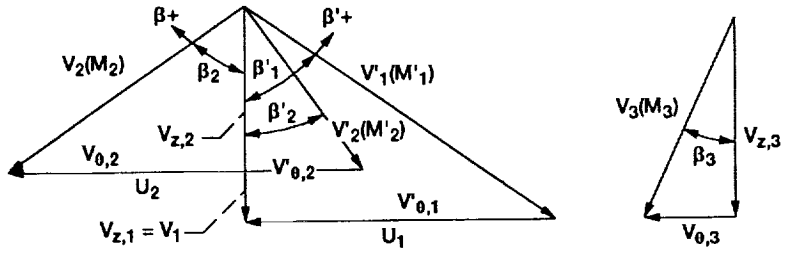

(b) Stage velocity diagram.

Figure 1.—Schematic presentation of symbols.

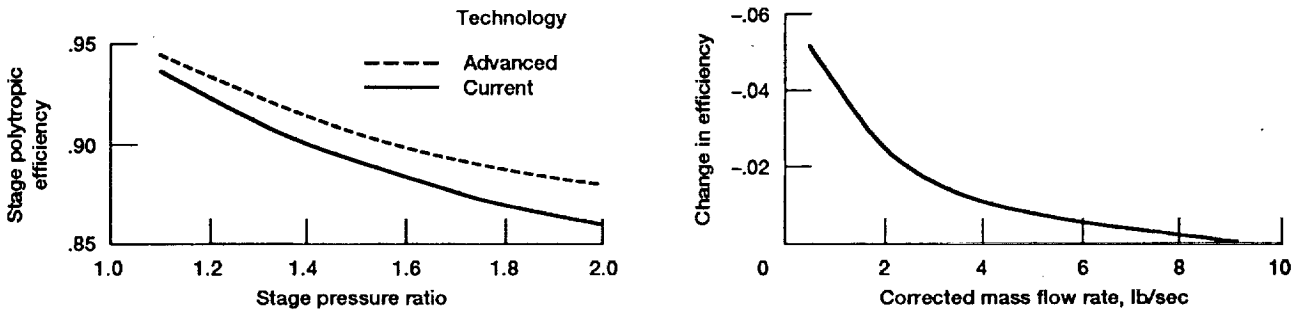

(a) Effect of stage pressure ratio.

(b) Size correction.

Figure 2.—Axial-flow compressor efficiency.

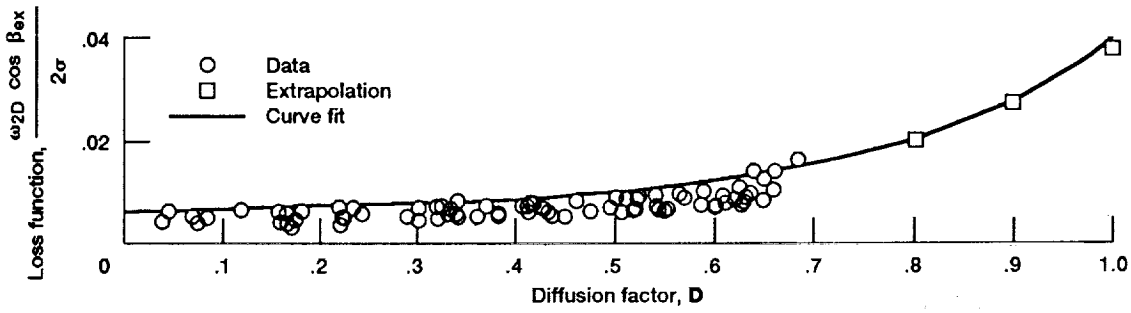

Figure 3.—Variation of loss function with diffusion factor.

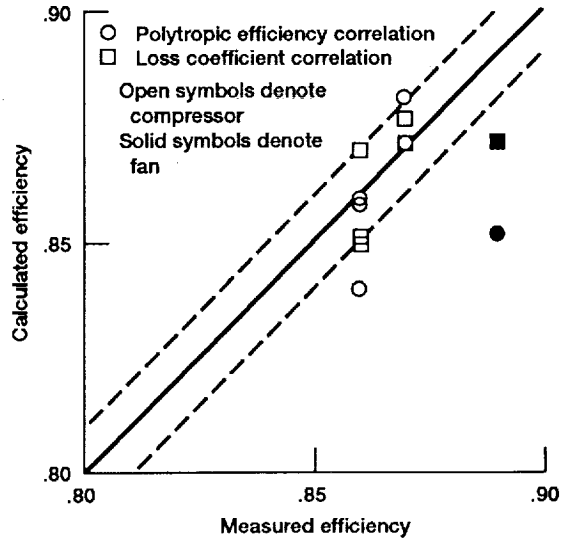

Figure 4.—Comparison of measured and calculated efficiencies.

REPORT DOCUMENTATION PAGE

Form Approved
OMB No. 0704-0188

1. AGENCY USE ONLY *(Leave blank)*	2. REPORT DATE	3. REPORT TYPE AND DATES COVERED
	July 1992	Final Contractor Report

4. TITLE AND SUBTITLE
Users Manual for Updated Computer Code for Axial-Flow Compressor Conceptual Design

5. FUNDING NUMBERS
WU-505-69-50

6. AUTHOR(S)
Arthur J. Glassman

7. PERFORMING ORGANIZATION NAME(S) AND ADDRESS(ES)
University of Toledo
Toledo, Ohio 43606

8. PERFORMING ORGANIZATION REPORT NUMBER
E-7003

9. SPONSORING/MONITORING AGENCY NAMES(S) AND ADDRESS(ES)
National Aeronautics and Space Administration
Lewis Research Center
Cleveland, Ohio 44135-3191

10. SPONSORING/MONITORING AGENCY REPORT NUMBER
NASA CR-189171

11. SUPPLEMENTARY NOTES
Prepared for Lewis Research Center, under Grant NAG3-1165. Arthur J. Glassman, University of Toledo, Toledo, Ohio 43606. Responsible person, John K. Lytle, (216) 433-7019.

12a. DISTRIBUTION/AVAILABILITY STATEMENT
Unclassified - Unlimited
Subject Category -61

12b. DISTRIBUTION CODE

13. ABSTRACT ***(Maximum 200 words)***
An existing computer code that uses a rapid approximate design methodology to determine the flow path for an axial-flow compressor was modified for use in air-breathing engine conceptual design studies. This code determines either the overall pressure ratio achievable in a given number of stages or the number of stages required for a given pressure ratio. The modifications make the code more applicable to the conceptual study of engine compressors. This report serves as the users manual for the modified code, which is named CSPAN. The changes made to the code and detailed descriptions of the code's input and output are presented in this report.

14. SUBJECT TERMS
Axial compressor

15. NUMBER OF PAGES
22

16. PRICE CODE
A03

17. SECURITY CLASSIFICATION OF REPORT	18. SECURITY CLASSIFICATION OF THIS PAGE	19. SECURITY CLASSIFICATION OF ABSTRACT	20. LIMITATION OF ABSTRACT
Unclassified	Unclassified	Unclassified	